

IMPEDANCE STUDY OF THIN PANI LAYERS OF DIFFERENT THICKNESSES

M. Žic, M. Kraljević Roković, L.J. Duić

Faculty of Chemical Engineering and Technology, University of Zagreb, 10000 Zagreb, Croatia

ABSTRACT

The effect of the polyaniline (PANI) layer thickness on impedance characteristics has been investigated. It has been found that PANI layer thickness has a significant influence on the impedance response of the PANI layer. The impedance response of PANI layers, presented in the low frequency region of Nyquist spectra, indicates an increase of real and imaginary impedance values as PANI layer thickness increases. Presentations of EIS data in Bode diagrams suggest two separate processes detected in the low and in the high frequency regions, respectively. The model used to analyze EIS data in terms of an electrical equivalent circuit resulted in PANI capacitance and PANI resistance values used, to calculate time constants for each of the processes. The EIS parameters, obtained from EIS data analysis, were used to interpret processes taking place inside PANI and at the PANI | electrolyte interface. The two major processes have been identified. The EIS analysis parameters are used to explain the changes of the PANI layer structure and of the PANI | electrolyte interface. In this work the total PANI layer capacitance, calculated from PANI EIS parameters, was compared to PANI current obtained by scanning the layer in the supporting electrolyte. The total PANI layer capacitance, in the potential region where the conductive form of PANI is present, was calculated as a function of two capacitances in series.

Keywords: electrosynthesis, PANI, electrochemical impedance spectroscopy, polymer layer structure.

1. INTRODUCTION

Polyaniline (PANI) can be synthesized by either a chemical or an electrochemical polymerization of aniline [1,2]. Chemically polymerized PANI layer has been studied for stainless steel corrosion protection [3], as a cathodic material for batteries [4-7], and for sensors [8,9]. The electrochemical synthesis of PANI offers the possibility to analyse PANI layer directly on the substrate grown, in precisely chosen conditions, and also to escape the possible mixture of counter-ions which are present in chemical synthesis [2,10]. PANI shows a catalytic effect for several redox reactions [10-12] under conditions where a conductive form of PANI is present. The electrochemical synthesis also makes it possible to control the rate of the polymerization by controlling the switching potential and the scan rate, and through that the thickness of the layer is controlled. The resulting layer can be easily studied by electrochemical techniques, including the electro-chemical impedance spectroscopy (EIS). The possibility of PANI to change the capacitance and resistance in respect to the applied potential is well known, so EIS has been used to determine the impedance parameters of PANI layers [13-20]. Constant phase elements (CPE) were used in order to describe the porosity of PANI layer, however they often have no clear physical meaning [14-17]. Many authors have used electrical equivalent circuit (EEC) to analyze impedance response of PANI layers [14, 15, 18]. EEC usually consists of two, or more, rc - circuits, which describe the impedance response of PANI layer. However, it is well known that several models EEC can fit a set of experimental data. When EEC is applied, it should physically describe the system under the investigation.

If the EEC has no "physical" meaning, or if there are no other supporting facts, results obtained by EEC analysis are doubtful.

An analysis of PANI layer impedance data gives the information on the resistivity and on the capacitance of PANI layer. To overcome the stability of the system during the measurements, as major limitations of the EIS, *Darowicki at al.* [14] used the dynamic electrochemical impedance spectroscopy (DEIS), a recently developed technique for impedance measurements. *Chi-Chang Hu at al.* [15] investigated PANI coated graphite electrodes by means of EIS. They describe an impedance response in the low and high frequency region as a consequence of the slow and fast exchange process governed by a counter-ions diffusion in PANI, and at PANI | electrolyte interface. *Gabrielli at al.* [19] interpreted counter-ions diffusion inside PANI layer as essential for maintaining the electroneutrality of PANI which can be disturbed by electrons entering/leaving the electrode as a consequence of the redox process in the layer. *Rossberg at al.* [20] considered the transfer of counter-ion from the electrolyte solution into PANI essential for the charge compensation. *Rubinstein at al.* [18] suggested that PANI behaves like a single homogenous phase, represented by a combination of double-layer capacitance and faradaic pseudocapacitance, which are associated with a fast electron-transfer process confined to the film, and which are potential dependent.

The influence of the applied potential on the impedance response of PANI layer was detected and described [14, 15]. It was found that the application of more positive potentials results in a decrease of imaginary impedance values in the low frequency region, which indicates an increase of the PANI capacitance. However, the possible changes of the PANI layer structure, which are caused by the applied potential change, were not discussed. The influence of the applied potential and of PANI layer thickness on the ionic charge-transfer resistance, responsible for the charge compensation inside PANI, was not explained.

The aim of this work was to investigate PANI impedance response in dependence of different thicknesses of PANI layers, to test the impedance model, and to explain the influence of the applied potential value on the impedance response of the PANI layer, *i.e.* on the EIS parameters. The response of PANI layer, obtained by cyclic voltammetry (CV), is compared to capacitance values calculated by EIS parameters.

2. EXPERIMENTAL

The electrochemical synthesis of PANI layers, as well as EIS measurements were carried out in a standard one-compartment cell. The working electrode was a Pt-disc ($A = 0.07 \text{ cm}^2$), a Pt-foil ($A = 0.5 \text{ cm}^2$) was used as an auxiliary electrode, whereas Ag/AgCl (3 mol dm^{-3} KCl) served as the reference electrode. PANI layers were synthesised by means of cyclic voltammetry (CV) from 0.5 mol dm^{-3} aniline in 3 mol dm^{-3} H_3PO_4 solution. The potential range of the synthesis was from -200 to 1000 mV vs. the reference electrode, at the scan rate $v = 50 \text{ mVs}^{-1}$. All the measurements were carried out at constant temperature, $t = 25 \pm 1 \text{ }^\circ\text{C}$. PANI layers were grown for a predetermined number of potential cycles (1-5) and designated as PANI1-PANI5. The influence of PANI layer thickness on the redox-reaction of 0.01 mol dm^{-3} hydroquinone/quinone ($\text{H}_2\text{Q/Q}$) was examined by means of CV in 3 mol dm^{-3} H_3PO_4 supporting electrolyte. EIS measurements were carried out using PAR Model 1025 Frequency Response Detector and PowerSuite software. In this work, the potential amplitude of the superimposed ac signal was 5 mV and the frequency range was from 0.01 Hz to 100 kHz. The measurements were performed at two potential values (530 and 400 mV).

3. RESULTS AND DISCUSSION

3.1. Electrochemical synthesis

Figure 1 compares voltammograms of PANI layers obtained for a different number of potential cycles. Voltammograms obtained for 3, 4, and 5 potential cycles show well developed current peaks, typical for PANI: A/A' representing leucoemeraldine/emeraldine

(LE/EM) and C/C' representing emeraldine/pernigraniline (EM/PG) transformations. Current peak C contains also superimposed aniline monomer oxidation current. Middle peaks (B/B' and B'/B), assumed to represent a side product and/or hydrolysis products [21], are also shown in Fig. 1. As PANI layer thickness increases, current peaks A/A' and C/C' increase as shown in Fig. 1.

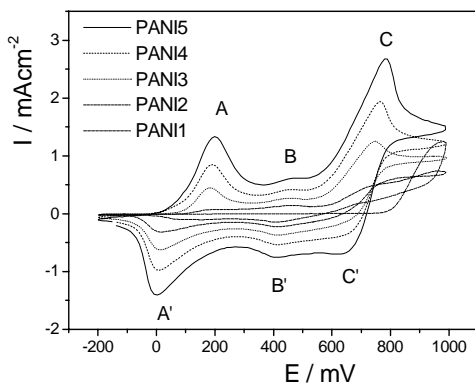


Fig. 1. Voltammograms of different thicknesses PANI layers in 0.5 mol dm^{-3} aniline solution

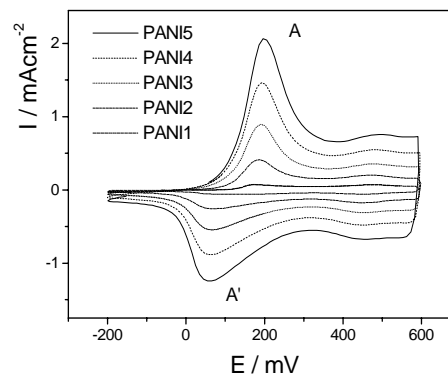


Fig. 2. Voltammograms of different thicknesses of PANI layers in 3 mol dm^{-3} H_3PO_4 solution.

Figure 2 compares voltammograms taken for different thicknesses of PANI layers in pure supporting electrolyte within the potential range from -200 to 600 mV. The potential window from 350 to 600 mV is the range of EM form of PANI. The capacitance behaviour in this potential range is assumed to be a characteristic of the PANI | electrolyte interface and of the PANI layer capacitance [2, 18].

3.2. Catalytic effect testing

In order to investigate the increase of a real surface area of PANI | electrolyte interface as PANI layer thickness increases, $\text{H}_2\text{Q}/\text{Q}$, redox-reaction was carried out at different thicknesses of PANI layers by means of CV. The quasi-reversible $\text{H}_2\text{Q}/\text{Q}$ redox-reaction has been studied by many authors [10-12]. The catalytic test has shown to be very useful in PANI morphology investigation [22]. The catalytic effect has been explained by adsorption of H_2Q molecules onto active PANI centres, *i.e.* on the protonated bipolaron form of PANI. According to Matveeva [12], bipolaron form of PANI is engaged in the adsorption of H_2Q molecules. It is assumed that the active PANI centres are homogeneously distributed on the PANI surface.

Therefore, it is expected that an increase of the PANI | electrolyte interface surface area will result in an increase of the active PANI centres. Figure 3 shows H_2Q oxidation current peak value as a characteristic of PANI layer thickness. There is a quite pronounced difference in current peak values obtained for different thicknesses of PANI layers. An increase of H_2Q oxidation current peak indicates also, an increase of PANI active centres, which can be attributed to an increase of the PANI | electrolyte surface area. The PANI | electrolyte surface area influences PANI electrochemical behaviour, when investigated by EIS. Therefore, in order to investigate the capacitance and resistance characteristics of different thickness PANI layers, EIS measurements were performed

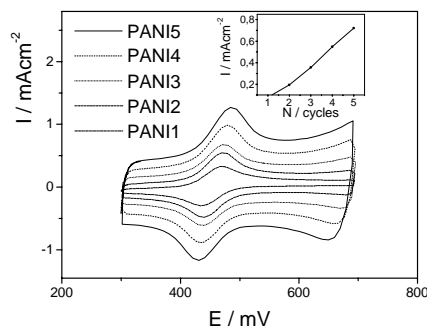


Fig. 3. The influence of different thicknesses of PANI layers on the current peak value of hydroquinone oxidation ($c_{\text{H}_2\text{Q}} = 0.01 \text{ mol dm}^{-3}$).

3.3. EIS measurements

3.3.1. Elemental description of EIS data

The Nyquist impedance spectra for different thicknesses of PANI layers measured at 530 and 400 mV are shown in Figs. 4 and 5, in which several features need to be described. Firstly, in the high frequency region of the Nyquist spectra, all curves for different layer thicknesses have a similar behaviour.

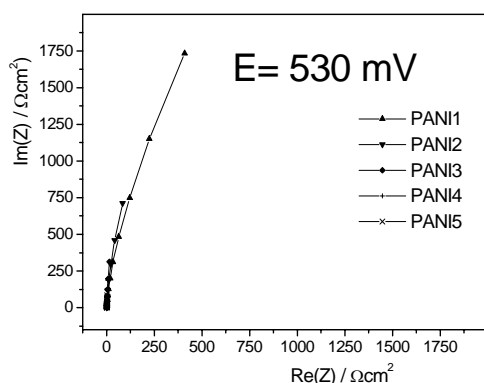


Fig. 4. Nyquist impedance spectra of different thicknesses of PANI layers.
 $E = 530 \text{ mV}$.

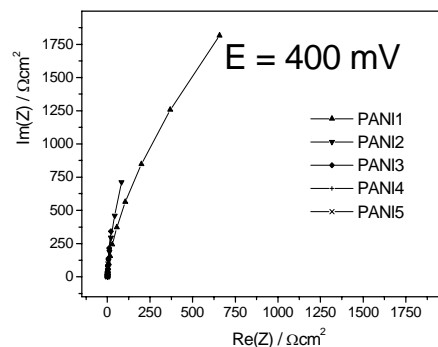


Fig. 5. Nyquist impedance spectra of different thicknesses of PANI layers.
 $E = 400 \text{ mV}$.

However, in the low frequency region of the Nyquist spectra there is an apparent difference between the impedance responses of different PANI layers.

The impedance response of PANI layers in the low frequency region suggests a typical PANI capacitive behaviour. Secondly, a decrease of the imaginary impedance value of the Nyquist spectra indicates an increase of PANI capacitance as the PANI layer thickness increases. Therefore, it is obvious that PANI layer thickness influences the real and imaginary impedance values in the low frequency region. The Bode diagrams for different PANI layer thicknesses at 530 and 400 m are given in Figs. 6 - 7.

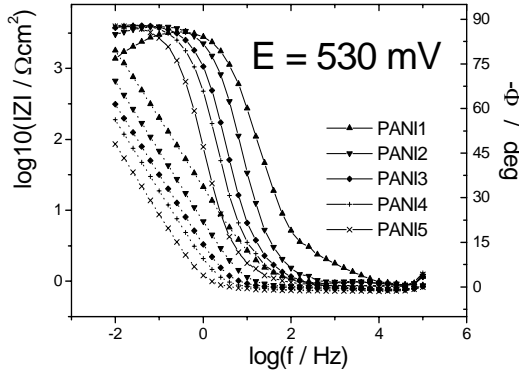


Fig. 6. Bode impedance spectra of different thicknesses of PANI layers.
E = 530 mV.

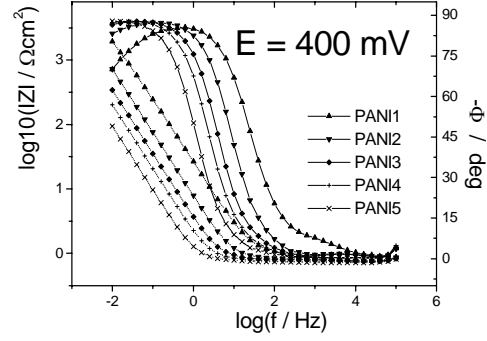


Fig. 7. Bode impedance spectra of different thicknesses of PANI layers.
E = 400 mV.

Phase angle vs. $\log(f/\text{Hz})$ dependence suggests two processes: one process in the low, and the other in the high frequency region. Results published earlier [15, 19] indicate that the high frequency region is attributed to the double layer charging and discharging processes, followed by the counter-ions exchange process at PANI | electrolyte interface.

The main difference in the phase angle vs. $\log(f/\text{Hz})$ dependence for the investigated different thicknesses of PANI layers is in the low frequency region of the Bode spectra. The low frequency region is attributed to the slow process of PANI bulk redox transition [15, 19]. An increase of the PANI layer thickness shifts the impedance data to a lower frequency region, as a result of a slow process decrease. The redox processes inside PANI, detected by EIS, are caused by 5 mV perturbation signal. These redox processes inside PANI layer are followed by an ingress/expulsion process of counter-ions. The electroneutrality of PANI layer is achieved by the fluxes of counter-ions, which diffuse through PANI and the PANI | electrolyte interface, balancing the electrons which enter/leave the electrode due to redox process of PANI [19]. The impedance response of PANI layers of different thicknesses, presented in the Bode spectra, suggests two time-constants, corresponding to the low and high frequency region. The two time-constants are described by two electrical circuits in a series (Fig. 8).

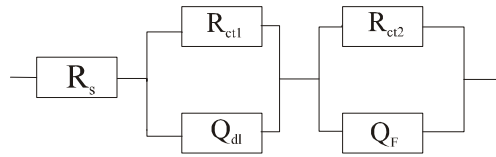


Fig. 8. Electrical equivalent circuit used to fit the impedance data.

The analysis of $Z(\omega)$ for investigated PANI layers is based on the following equations, similar to the reported ones [14, 15]:

$$Z(\omega) = R_s + Z_I(\omega) + Z_F(\omega) \quad (1)$$

$$1/Z_I(\omega) = 1/R_{ct1} + j\omega C_{dl} \quad (2)$$

$$1/Z_F(\omega) = 1/R_{ct2} + j\omega C_F \quad (3)$$

where ω , R_s , Z_I , Z_F , R_{ct1} , R_{ct2} , C_{dl} and C_F are angular frequency, solution resistance, impedance of PANI | electrolyte interface, bulk faradic impedance, ionic charge-transfer resistance at PANI | electrolyte interface, ionic charge-transfer resistance in the PANI layer, double-layer

capacitance and bulk faradic pseudocapacitance, respectively. Z_l indicates impedance of PANI | electrolyte interface and it is interpreted as a double-layer capacitance (C_{dl}) in series with an ionic-charge transfer resistance R_{ct1} . Bulk faradic impedance (Z_F), *i.e.* the bulk redox transition of the PANI layer, is explained as a pseudocapacitance of the PANI layer in parallel to resistor R_{ct2} . The layers investigated were in the same form of PANI, *i.e.* EM, therefore, the impedance analysis, for all the layers, is based on the previously specified equation (1). The system has shown deviations from the ideal behaviour, and therefore constant phase elements (*CPE*) were used instead of a double-layer (C_{dl}) capacitance and bulk faradic pseudocapacitance (C_F). Transfer function (1) for electrical equivalent circuit (Fig. 8) was modified, and transfer function (4) was used in order to analyze EIS PANI data. The admittance of *CPE* is defined as $Q(j\omega)^n$, where Q is a constant of following dimensions $(Fs)^n \text{ cm}^{-2}$, and exponent n is related to the slope of $\log(Z)$ vs. $\log(f/Hz)$ plot, respectively. The constant phase element value, for $n = 1$, becomes pure capacitance. ZSimpWin software from Princeton Applied Research was used to obtain the electrochemical parameters from equation (4):

$$Z(\omega) = R_s + \frac{1}{1/R_{ct1} + Q_{dl}(j\omega)^n} + \frac{1}{1/R_{ct2} + Q_F(j\omega)^n} \quad (4)$$

where ω , R_s , R_{ct1} , R_{ct2} , $Q_{dl}(j\omega)^n$ and $Q_F(j\omega)^n$ are angular frequency, solution resistance, ionic charge-transfer resistance at PANI | electrolyte interface, ionic charge-transfer resistance in the PANI layer, the admittance of double-layer constant phase element, and the admittance of bulk faradaic constant phase element, respectively. The fitting parameters were accepted if χ^2 value was below 10^{-4} , and they are given in Tabs. 1 - 2. Solution resistance (R_s) does not show dependence neither on the potential nor on angular frequency, nor on the PANI layers thickness, which is in agreement with equation (4). Since the supporting electrolyte and the distance between the working and the reference electrode during the measurements were kept constant, there was no reason for R_s value to vary. However, Q_{dl} and Q_F indicate the dependence on the PANI layer thickness. The influence of the applied potential on PANI pseudocapacitance indicates higher Q_F values at 530 mV, compared to those obtained at 400 mV. Low n_{dl} values implicate the roughness of PANI | electrolyte interface and therefore the use of *CPE* is justified [15, 20]. The n_f value is shifting towards $n = 1$ value as PANI layers thickness increases, suggesting that PANI pseudocapacitance (Q_F) is approaching the ideal capacitance values.

3.3.2. EIS model testing

There are many EEC which can fit a set of experimental data and this way of investigating PANI layer of different thicknesses offers the possibility to test proposed EEC. Applying this method, it is possible to predict the behaviour of some parameters. It is assumed that faradaic redox process (C_F) and the PANI | electrolyte interface (C_{dl}) increases as the PANI layer thickness increases, therefore, the EIS parameters results (C_F and C_{dl}) should increase as the PANI layer thickness increases. If EIS model behaves in that way like mentioned above, this should be the additional supporting fact, besides χ^2 value, for using the propose EEC.

The impedance model (Fig. 8) is tested by comparing Nyquist spectra (Fig. 4 - 5) with the impedance parameters presented in Tabs. 1 - 2. The same trend, *i.e.* an increase of PANI capacitance values in the low frequency region, is presented in the Nyquist spectra and obtained by the impedance model. The increase of PANI | electrolyte interface capacity, calculated by EIS, as PANI layer thickness increases, is confirmed by the increase of H₂Q oxidation current (Fig. 3).

N / cycles	$R_s/\Omega\text{cm}^2$	$Q_{dl}/(\mu\text{F})^n \text{cm}^{-2}$	n_{dl}	$R_{ct1}/\Omega\text{cm}^2$	$Q_F/(\mu\text{F})^n \text{cm}^{-2}$	n_F	$R_{ct2}/\Omega\text{cm}^2$
1	0,703	0,060	0,496	0,606	0,007	0,972	8283
2	0,812	0,176	0,752	0,078	0,023	0,992	7536
3	0,802	0,165	0,893	0,074	0,050	0,995	6484
4	0,745	0,414	0,698	0,106	0,084	0,998	5223
5	0,735	0,673	0,714	0,084	0,183	0,996	2752

Table 1. Values obtained by impedance analysis of different thicknesses of PANI layers at 530 mV

N / cycles	$R_s/\Omega\text{cm}^2$	$Q_{dl}/(\mu\text{F})^n \text{cm}^{-2}$	n_{dl}	$R_{ct1}/\Omega\text{cm}^2$	$Q_F/(\mu\text{F})^n \text{cm}^{-2}$	n_F	$R_{ct2}/\Omega\text{cm}^2$
1	0,755	0,009	0,727	0,269	0,006	0,962	6022
2	0,809	0,128	0,824	0,062	0,020	0,987	6872
3	0,789	0,184	0,799	0,077	0,045	0,991	7040
4	0,753	0,248	0,834	0,083	0,077	0,993	5558
5	0,727	0,773	0,642	0,090	0,166	0,993	4404

Table 2. Values obtained by impedance analysis of different thicknesses of PANI layers at 400 mV.

Figures 9 - 10 represent capacitance of PANI | electrolyte interface (C_{dl}) and PANI pseudocapacitance (C_F) as a function of PANI layer thickness, calculated from the data presented in Tabs. 1 - 2 and equation (5) [23];

$$C = Q(QR)^{\frac{1-n}{n}} \quad (5)$$

where C is pseudocapacitance, Q is constant phase element, R is a resistor in parallel, and exponent n is related to the slope of $\log(Z)$ vs. $\log(f)$ plot, respectively.

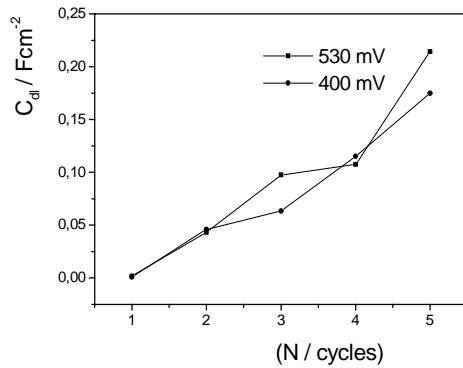


Fig. 9. Influence of PANI layer thickness on PANI | electrolyte interface capacitance

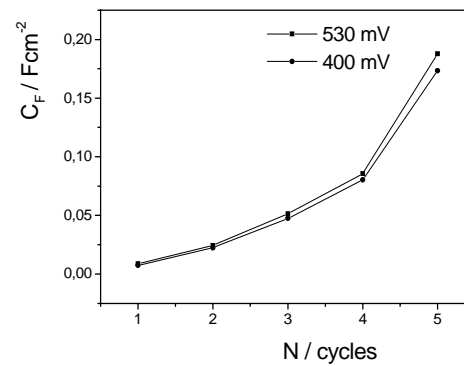


Fig. 10. Influence of PANI layer thickness on PANI pseudocapacitance

It is very interesting to calculate pseudocapacitance value for exponent $n = 1$. The right side value of equation (5), for $n = 1$ becomes pure capacitance. From Figs. 9 - 10 it is obvious that C_{dl} and C_F values show an increase as PANI thickness increases, indicating a higher C_{dl} values compared to C_F values. But, as shown in Fig. 10, C_F vs. N suggests the exponential growth, *i.e.* C_F value exceeds C_{dl} value after a certain thickness has been achieved.

3.3.3. Influence of PANI layer thickness and applied potential to the PANI structure

The applied potential influence on faradaic process was previously investigated by Rossberg *at al.* [20]. They found that faradaic process is of continuous nature, but the possible changes in PANI structure, due to potential change, were not discussed.

The influence of the applied potential on C_F , shown in Fig. 10, indicates an increase of C_F value as the potential increases. A greater exchange of counter-ion process inside PANI is detected by EIS, and it is explained as a consequence of an increase of C_F value, which leads to higher population of free sites in PANI [19]. Therefore, during the PANI layer oxidation, from 400 to 530 mV, a transformation to a higher population of quinoidal units takes place, and changes the PANI layer structure. Gabrielli *et al.* [19] found that higher potential leads to a mass increase, detected by ac electrogravimetry. They showed that anions, cations and solvent are involved in charge compensation during the reduction/oxidation of PANI, all being potential dependent, but, the possible potential influence on PANI structure was not considered.

The C_F increase must be followed by a change in the structure of PANI layer. Quinoidal units, introduced during the oxidation process, cause a more rigid form of PANI chains, which inhibit the rotation of polymer chains [24], due to the double bond effect. This leads to a lower number of possible chain conformations. An increase of PANI free volume, associated with the polymer chain conformation [25], as a result of a higher population of quinoidal units, is expected. Therefore, PANI layer structure changes with the change of the applied potential, and the application of different EIS signals (different DC component) results in different EIS data and parameters, as shown in the Figs. 4-7 and Tabs. 1-2.

PANI layer thickness, as well as the applied potential influence on C_{dl} values, is given in Fig. 9. An increase of C_{dl} values is detected with the increase of PANI layer thickness. The change of PANI layer structure, *i.e.* the change of PANI free volume, induces also the change of PANI | electrolyte interface surface area. As more positive potential is applied, the roughness factor (lower n_{dl} values) of the surface increases, indicating an increase of PANI | electrolyte interface capacitance, which is detected by the EIS (Tabs. 1-2).

3.3.4. The PANI structure influence on charge compensation resistance

Two counter-ion exchange processes, required to obtain the electroneutrality of PANI, are governed by two charge-transfer resistances (R_{ct1} and R_{ct2}). It is fair to assume that a slower counter-ions exchange process will result in an increase of charge-transfer resistance value. Counter-ions exchange process within the PANI layer provides a higher resistance (R_{ct2}) for charge compensation, compared to the charge compensation resistance (R_{ct1}) at PANI | electrolyte interface [15]. The same trend is obtained by EIS analysis, indicating greater R_{ct2} comparing to R_{ct1} values (Tabs. 1 - 2).

The change of the PANI layer structure has an influence on a counter-ion process inside the PANI layer, and that change results in R_{ct2} value change. Therefore, an influence of the applied potential on R_{ct2} value is expected. A decrease of R_{ct2} value, as more positive potential is applied, indicates an easier counter-ion exchange process inside the PANI layer. Thus, the values in Tabs. 1 - 2 describe the PANI layer as an ion-exchange [19] membrane, the ion-exchange properties of which, increase with the more positive potential applied.

Counter-ion exchange process inside the PANI layer, described by the R_{ct2} value, is facilitated as PANI layer thickness increases (Tabs 1 - 2). It is fair to assume that also a decrease of R_{ct2} , leads to PANI free volume increase. PANI free volume increase can be explained as a consequence of a higher population of quinoidal units inside the PANI layer.

It is found that the applied potential and PANI layer thickness have an influence on the counter-ions exchange process and, consequently on R_{ct2} value. Also, a direct connection between the counter-ions exchange process and charge compensation resistance is confirmed. It is interesting to notice that the applied potential and PANI layer thickness have no significant effect on R_{ct1} compared to R_{ct2} value (Tabs. 1 - 2). This effect shows, that the counter-ion exchange process at PANI | electrolyte interface is not influenced by PANI chain structure, and therefore there is no reason for R_{ct1} value to vary with the applied potential, or with the PANI layer thickness changes.

3.3.5. The time-constant calculation

From data presented in Tabs. 1 – 2, it is possible to calculate time-constants (rc) for each of the processes. As mentioned above, two time-constants are used to describe the fast (rc_{dl}) and slow processes (rc_F), detected by EIS in the high and low frequency region.

The values for time constants (Figs. 11 and 12) show an increase as PANI thickness increases. Figures. 6 – 7 show an increase of time-constant value (rc_F) as a shift of impedance data. It is obvious that the shift of rc_F time-constant is more pronounced, compared to rc_{dl} shift, which suggests a greater influence of PANI layer thickness on rc_F . Resulted rc-constants, which correspond to experimental data (Figs. 6 - 7), show that application of proposed EEC is justified.

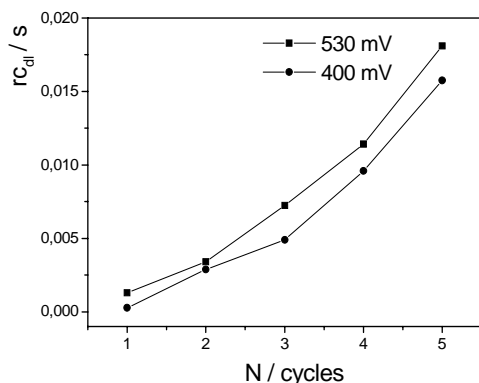


Fig. 11. Influence of PANI layer thickness on the rc_{dl} time-constant.

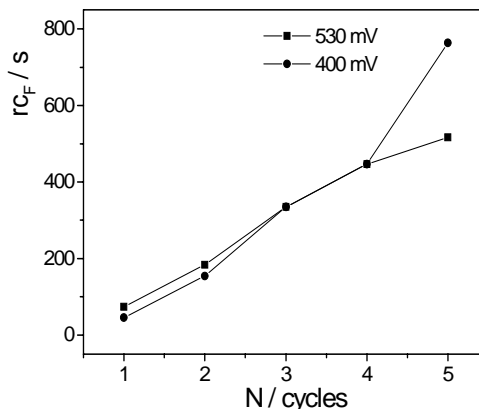


Fig. 12. Influence of PANI layer thickness on the rc_F time-constant.

3.3.6. The origin of capacitive current plateau

The capacitive current plateau is an important aspect of PANI electrochemistry. The origin of this process is not well understood. It was explained that continuous faradaic charge transfer has influence on capacitive current plateau [20]. It is well known that electroactive behaviour of PANI is explained through two process, i.e. process inside PANI and at PANI | electrolyte interface [26, 27]. Therefore, the influence of PANI | electrolyte interface, on current detected by CV, is discussed. There must be some connection between faradaic and PANI | electrolyte interface capacitance, responsible for capacitive current plateau. We present here some insight in capacitive current plateau origin.

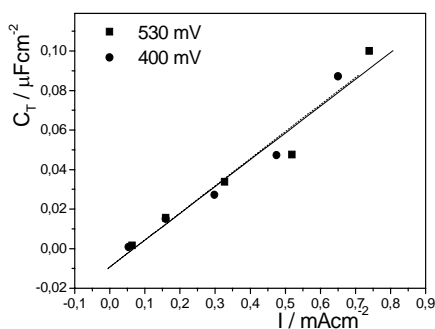


Fig. 13. Influence of PANI current on total serial capacitance

Current in the potential region where conductive form of PANI (EM) is present (350 to 600 mV), is a consequence of a charge change in time ($I=\Delta Q/\Delta t$) due to the redox process of the PANI layer, and due to PANI | electrolyte interface charging/discharging process. It is very important to notice that current values within EM potential region do not depend on the applied potential change, and that represents typical capacitive behaviour. Thus, the shape of the voltammograms presented in Figs. 1 - 2 suggests that the total capacitance (C_T) is responsible for polymer behaviour in the conductive form of PANI. From the data presented in Figs. 9 - 10 it is possible to calculate C_T value as a function of two serial capacitances (C_{dl} and C_F), according to equation (4) and Fig. 8. C_T values of different PANI layer thicknesses at 530 and 400 mV can be presented as a function of PANI current. Current values are taken from the voltammograms in Fig. 2. Figure 13 shows C_T of PANI layers as a function of the PANI current at 530 and at 400 mV. Since the current corresponds to the PANI layer thickness, an increase of the C_T value is expected with the current increase. It is obvious that C_T of PANI layer is, as shown in Fig. 13, a linear function of PANI current with the same slope values at 530 as well as at 400 mV, which means that PANI capacitance in that potential region is C_T governed. This indicates that both electrochemical techniques, CV and EIS, are sensitive to PANI pseudocapacitance and PANI | electrolyte interface capacitance as well. The validity of the impedance model used to analyse PANI EIS data is once more confirmed by the obtained C_{dl} and C_F values which were used to calculate C_T presented in Fig. 13.

4. Conclusion

An impedance response of the PANI layer, in the low and high frequency regions, is explained as a consequence of an counter-ions exchange process inside the PANI layer and at the PANI | electrolyte interface, which are both required to maintain the electroneutrality of PANI. The Nyquist diagrams in the low frequency region show a decrease of imaginary and real impedance values as PANI layer thickness increases. EIS analysis of electrochemically deposited thin PANI layers shows an increase in faradaic (C_F) pseudocapacitance, and in PANI | electrolyte interface capacitance (C_{dl}) value as PANI layer thickness increases. An increase of PANI | electrolyte surface area, as a thicker PANI layer is obtained, is confirmed by an increase of H₂Q oxidation current peak.

There is no method reported which is used to analyse PANI in order to obtain information which are used to predict or test EEC. Here, we propose an approval of PANI investigation which is based on investigation of different thicknesses PANI layers. The electrochemical behaviour of PANI is governed by the process which occurs inside PANI and at PANI | electrolyte interface. The EEC results must correspond to faradaic redox process (C_F) and the PANI | electrolyte surface (C_{dl}) increase as the PANI layer thickness increases. The increase of the PANI layer thickness leads to an increase of the faradaic process, *i.e.* the slow counter-ions exchange process, detected by EIS. The increase of the PANI | electrolyte interface capacitance, *i.e.* increase of the fast counter-ion exchange process, is explained through a test on catalysis [10-12] and it is detected by EIS. If all EIS parameters (C_F and C_{dl}) show an increase as the PANI layer thickness increases, it is assumed that proposed application of EIS model is justified.

According to the impedance response of the PANI layer, presented in the Bode spectra, two processes are identified, and two time-constants are calculated. The influence of the applied potential on PANI (C_F) pseudocapacitance and PANI | electrolyte interface capacitance (C_{dl}) is explained. It is suggested that a higher population of quinoidal units is obtained in the PANI layer when a more positive potential is applied. The changes of PANI layer structure, as a consequence of a transformation to quinoidal units are explained by PANI free volume increase. A decrease of R_{ct2} value as PANI thickness increases is detected and also explained as PANI free volume increase. EIS parameters were used to describe the change of PANI layer structure, which occurs when applying a more positive potential or when investigating a thicker PANI layer. Time constants of each circuit (rc) are calculated and their influence to Bode spectra is explained.

Important aspect of conductive PANI property is the existence of a capacitive current plateau in the cyclic voltammogram. A novel fundamental insight, involving the origin of capacitive current plateau, is proposed. The total serial capacitance of the PANI layer (C_T) has been defined, calculated and compared to the PANI current obtained by potential scanning of the PANI layer in the supporting electrolyte. C_T and PANI current dependences have been described as linear, indicating an ideal PANI capacitance behaviour in the potential region, where conductive form of PANI is present. The investigation of PANI using CV and EIS indicates that these electrochemical techniques are sensitive to both PANI pseudocapacitance and PANI | electrolyte interface capacitance.

Acknowledgment

The financial support from the Ministry of Science of the Republic of Croatia under the 0125-010 grant is gratefully acknowledged.

References:

1. Y. Wei, J. Wang, X. Jia, Jui-Ming Yeh.: *Polymer* **36** (23) (1995) 1995.
2. M. Geniès, *J. Electroanal. Chem.*: **283** (1990) 205.
3. B. Wessling, *Adv. Mater.* **6** (3) (1994) 226.
4. Wallace G. G.; Spinks, G. M.; Kane-Maquirie, L. A. P.: Teasdale, In *Conductive Electroactive Polymers*; Chapter 1, pp 9 - 49, P. R, Eds; CRC Press: Boca Raton, FL, 2003;
5. N. Li, J. Y. Lee, L. H. Ong.; *J. Appl. Electrochem.* **22** (1992) 512 – 516.
6. T. Sotomura, H. Uemachi, K. Takeyama, K. Naoi, N. Oyama.; *Electrochim. Acta* **37** (1992) 1851 – 1854.
7. N. L. D. Somasiri, A. G. Macdiarmid.; *J. Appl. Electrochem.* **18** (1988) 92 -95.
8. M. Shaolin, X. Huaiguo, Q. Bidong, *J. Electroanal. Chem.* **304** (1991) 7.
9. M. Shaolin, K. Jinqing, *Electrochim. Acta* **40** (1995) 241.
10. Z. Mandic, L. Duic, *J. Electroanal. Chem.*: **403** (1996) 133.
11. E. S. Matveeva.: *Synth. Met.* **83** (1996) 98-96.
12. E. S. Matveeva, I. Hernandez-Fuentes, V. Parkhutik, R. Diaz-Calleja.: *Synth. Met.* **83** (1996) 181-184.
13. S. K. Mondal, K. R. Prasad, N. Munichandraiah.: *Synth. Met.* **148** (2005) 275.
14. K. Darowicki, J. Kawula.: *Electrochim. Acta* **49** (2004) 4829.
15. Chi-Chang Hu, Chien-How Chu.: *J. Electroanal. Chem.* **503** (2001) 105.
16. G. Inzelt, G. Lang, V. Kertesz, J. Bacskai.: *Electrochim. Acta* **38** (1993) 2053.
17. G. Sandi, P. Vanysek.: *Synth. Met.* **63** (1994) 133.
18. I. Rubinstein, E. Sabatani, J. Rishpon.; *J. Electrochem. Soc.* **134** (1987) 3078.
19. C. Gabrielli, M. Keddam, N. Nadi, H. Perrot.: *J. Electroanal. Chem.* **485** (2000) 101.
20. K. Roßberg, G. Paasch, L. Dunsch, S. Ludwig.; *J. Electroanal. Chem.* **443** (1998) 49.
21. G. Zotti, S. Cattarin, N. Comisso.: *J. Electroanal. Chem.* **235** (1987) 259.
22. Lj. Duic, S. Grigic.; *Electrochim Acta* **46** (2001) 2795 – 2803.
23. ZSimpWin 3.10.
24. M. Kraljic Rokovic, Lj. Duic.; *Electrochim. Acta* , accepted for publication.
25. Kumins K., Kwei T. K.: *Free volume and other theories in Diffusion in polymers*, J. Crank and G. S. Park, Eds., Academic Press, London, 1968; Chapter 4, pp 107 - 140.
26. C. Deslouis, T. El Moustafid, M. M. Musiani, M. E. Orazem, V. Provost, B. Tribollet.: *Electrochim. Acta* **44** (1999) 2087 – 2093.
27. C. Gabrielli , J.J. Garcia-Jareno, H. Perrot.: *Electrochim.* **46** (2001) 4095–4103.